Spin-Spin Interaction Constants from the Hyperfine Structure of Pairs of Coupled Ions*

J. W. Culvahouse, D. P. Schinke,† and Larry G. Pfortmiller

Department of Physics and Astronomy, The University of Kansas, Lawrence, Kansas 66044

(Received 14 August 1968)

The hyperfine structure of pairs of paramagnetic ions with identical nuclear spins and a spin-spin interaction effectively of the form $K_0 S_1 \cdot S_2 + K_z S_1^z S_2^z$ is discussed. The structure of the spectra depends on the ratio $p = K_0/A$, and a general discussion of the key features of the spectra is given for p in the range zero to infinity. The technique by which the spin-spin interactions may be extracted from the spectra is demonstrated by four examples which correspond to p values of 2, 5.7, 11, and 48. In all cases K_z is sufficiently large that a major part of the hyperfine structure of the pairs is clear of the spectrum of the isolated ions. For the nearest-neighbor axial pairs of Pr^{3+} in $La_2(C_2H_5SO_4)_6 \cdot 9H_2O$, $K_0 = +0.467$ cm^{-1} and $K_z = -0.474$ cm^{-1}; for Pr^{3+} in $LaCl_3$, the nearest-neighbor axial pairs have $|K_0| = 2.44$ cm^{-1} and $|K_z| = 1.79$ cm^{-1}, where the z axis here and below is the interionic axis and the trigonal axis of the crystal. The other two examples are provided by Co^{2+} in the nearest-neighbor X sites of $La_2Mg_3(NO_3)_{12} \cdot 24H_2O$; one for the magnetic field along the interionic axis, and the other for the magnetic field perpendicular to this axis. One finds $K_0 = +0.105$ cm^{-1}, and $K_z = -0.170$ cm^{-1}.

I. INTRODUCTION

GENERALLY, in the study of spin-spin interactions by the pair technique, the presence of hyperfine interactions is considered an unwelcome complication. A notable exception is the situation in which the pairs are coupled by an isotropic exchange interaction $K_0 S_1 \cdot S_2$ which is much stronger than the hyperfine interaction $A I_1 \cdot S_1$. If the ions are identical, and of spin one-half, $S = S_1 + S_2$ and $S_z = S_1^z + S_2^z$ are diagonal in the singlet-triplet representation, and the hyperfine structure consists of $4I+1$ lines spaced at the interval $A/2g\beta$.[1] The center of the structure coincides with the center of the isolated ion spectrum (if the g factor of the pair is unchanged), and the intensity shows the familiar stairstep pattern: 1, 2, $\cdots$, $2I$, from the outside to the inside. If there is a dipolar interaction or anisotropic exchange, the coupled hyperfine interaction will split into two identical components shifted up and down from the isolated ion resonance by equal amounts on a magnetic field display. Spectra of this type have been analyzed many times,[2] and the variation of the relative intensity of the pair spectra and the isolated ion spectra with the temperature has served as an important source of information on large exchange couplings. In this paper we illustrate the extension of this technique to cases for which $K_0 \sim A$.

Baker[3] has also found hyperfine interactions useful in the analysis of Nd^{3+} spin-spin interactions in $La_2(C_2H_5SO_4)_6 \cdot 9H_2O$ (hereafter LES) where the spin-spin interaction is of the form $K_0 S_1 \cdot S_2 + K_z S_1^z \cdot S_2^z$. In that case,

one of the ions in a pair has a nonzero nuclear spin and the other a nuclear spin of zero so that the hyperfine interaction is asymmetric for the interchange of the ions and is strong enough to break the selection rule $\Delta S = 0$ for the coupled pair. The magnetic field position of the additional transitions allows a direct determination of K_0. This concept forms an important part of the present discussion and we extend it to the case where both ions have nuclei with spin. We limit the discussion to the case where both nuclear spins are the same. One still has the possibility that the selection rule $\Delta S = 0$ can be broken because the two ions are inequivalent when the projections of the nuclear spin on the quantization axis of the electron spin are different.

In Sec. II, we discuss the general case of two identical ions (including identical nuclei) which have a spin-spin interaction that is *effectively* of the form

$$K_0 S_1 \cdot S_2 + K_z S_1^z S_2^z. \tag{1}$$

Computed hyperfine structure patterns are given for a number of cases and key features of the spectra are pointed out.

In Sec. III, these results are applied to four widely different cases in which the ratio of K_0 to the diagonal part of the hyperfine interaction energy ranges from approximately two to about fifty. Two of the examples are Pr^{3+} in LES and $LaCl_3$. The other two examples are provided by a single type of ion pair, the nearest-neighbor Co^{2+} ions in $La_2Mg_3(NO_3)_{12} \cdot 24H_2O$ (hereafter LMN). In one example the magnetic field is along the symmetry axis of the crystal (which is also the interionic axis of the pair), and in the other example the magnetic field is perpendicular to this axis. There are actually two types of cobalt sites in the LMN lattice, the nearly cubic X site and the trigonal Y site. The nearest neighbor of an X site is another X site on the trigonal axis. It is only these pairs that are discussed in this paper, despite the fact that the interaction between ions in an X site and the nearest Y site is somewhat

† Present address: Bell Telephone Laboratories, Murray Hill, N. J.

[1] One of the early discussions of such hyperfine structure was given by C. P. Slichter, Phys. Rev. **99**, 479 (1955).

[2] Some more resent results from this type of measurement are reviewed by J. Samuel Smart, in *Magnetism III*, edited by George T. Rado and Harry Suhl (Academic Press Inc., New York, 1963).

[3] J. M. Baker, Phys. Rev. **136A**, 1341 (1964).

larger and because of the higher multiplicity of neighbors dominating the bulk properties of LaCoN. The nearest-neighbor X-Y interaction and other spin-spin interactions as well as the bulk properties of LaCoN will be discussed elsewhere.[4] The axial pair interactions reported here for Pr^{3+} are the dominant spin-spin interactions, and appear to account for the magnetic specific heat of PrES and $PrCl_3$; but the detailed discussion of this agreement and the physical source of the interaction will be given elsewhere.[5] The aim of this paper is to illustrate the utility of and the techniques for analysis of the hyperfine structure of pairs of equivalent ions.

II. THEORY

The Hamiltonian for two interacting ions, each of effective electron spin one-half and nuclear spin I, may be written in the form

$$\mathcal{3C} = \beta(\mathbf{H} \cdot \mathbf{g}_1 \cdot \mathbf{S}_1 + \mathbf{H} \cdot \mathbf{g}_2 \cdot \mathbf{S}_2)$$
$$+ \sum_{mm'} A_{mm'}(1) T_{1m}(I_1) T_{1m'}(S_1)$$
$$+ A_{mm'}(2) T_{1m}(I_2) T_{1m}(S_2)$$
$$+ \sum_{mm'} \mathcal{J}_{mm'}(1,2) T_{1m}(S_1) T_{1m'}(S_2), \quad (2)$$

where spherical tensor operators of rank one are defined as[6]

$$T_{11}(S) = -S_+/\sqrt{2}, \quad (3a)$$
$$T_{10}(S) = S_z, \quad (3b)$$
$$T_{1-1}(S) = S_-/\sqrt{2}. \quad (3c)$$

The Hermitian adjoint of these operators is given by $(T_{1m}(S))^\dagger = (-1)^m T_{1-m}(S)$, so that Hermiticity of (2) implies that

$$\mathcal{J}_{00} = \mathcal{J}_{00}^* = J_{00}, \quad (4a)$$

where J_{00} is real, and four other constraints:

$$\mathcal{J}_{1-1} = \mathcal{J}_{-11}^*, \qquad \mathcal{J}_{10} = -\mathcal{J}_{-10}^*,$$
$$\mathcal{J}_{01} = -\mathcal{J}_{0-1}^*, \qquad \mathcal{J}_{11} = \mathcal{J}_{-1,-1}^*, \quad (4b)$$

which is the well-known result that a general bilinear spin-spin interaction can contain at most nine independent constants. If an inversion center exists between the two ions, the spin-spin interaction coefficients must be symmetric in the interchange of the two ions, so that the number of independent constants is reduced to six by the relations

$$\mathcal{J}_{10} = \mathcal{J}_{01}, \quad (5a)$$

and

$$\mathcal{J}_{1-1} = \mathcal{J}_{-11} = J_{1-1}, \quad (5b)$$

where J_{1-1} is real. In this case $g_1 = g_2$; and we assume

[4] D. P. Schinke and J. W. Culvahouse (unpublished).
[5] J. W. Culvahouse and L. G. Pfortmiller (unpublished).
[6] A. R. Edmonds, *Angular Momentum In Quantum Mechanics* (Princeton University Press, Princeton, N. J., 1957).

that the two nuclei are identical, $I_1 = I_2$ and $A_{mm}(1) = A_{mm}(2)$. If the interionic axis coincides with a crystalline axis that is a symmetry axis of order three or higher, then only J_{1-1} and J_{00} can be nonzero, and (2) may be written in the form

$$\mathcal{3C} = g_{\parallel}\beta H_z(S_1^z + S_2^z) + g_{\perp}\beta[H_x(S_1^x + S_2^x)$$
$$+ H_y(S_1^y + S_2^y)] + A(I_1^z S_1^z + I_2^z S_2^z)$$
$$+ B(I_1^x S_1^x + I_2^x S_2^x + I_1^y S_1^y + I_2^y S_2^y)$$
$$+ K_0 \mathbf{S}_1 \cdot \mathbf{S}_2 + K_z S_1^z S_2^z, \quad (5)$$

where

$$K_0 = -J_{1-1}, \quad (6a)$$

and

$$K_z = J_{00} + J_{1-1}. \quad (6b)$$

If $B = 0$ and H is along the z axis, exact solution of the eigenvalue problem for the Hamiltonian (5) is quite simple. If one begins in the singlet-triplet representation of the electron spins and forms a simple product representation with the nuclear states, the basis states are

$$\psi_{11}(m_1, m_2) = |+\tfrac{1}{2}, +\tfrac{1}{2}\rangle |m_1, m_2\rangle, \quad (7a)$$
$$\psi_{1-1}(m_1, m_2) = |-\tfrac{1}{2}, -\tfrac{1}{2}\rangle |m_1, m_2\rangle, \quad (7b)$$
$$\psi_{10}(m_1, m_2) = (1/\sqrt{2})\{|\tfrac{1}{2}, -\tfrac{1}{2}\rangle + |-\tfrac{1}{2}, \tfrac{1}{2}\rangle\} |m_1, m_2\rangle, \quad (7c)$$
$$\psi_{00}(m_1, m_2) = (1/\sqrt{2})\{|\tfrac{1}{2}, -\tfrac{1}{2}\rangle - |-\tfrac{1}{2}, \tfrac{1}{2}\rangle\} |m_1, m_2\rangle, \quad (7d)$$

where $|\tfrac{1}{2}, \tfrac{1}{2}\rangle$, etc., is the product of eigenstates of S_i^z and $|m_1, m_2\rangle$ is a product of eigenstates of I_i^z. In this representation, the only nondiagonal matrix elements of (5) are between states $\psi_{10}(m_1, m_2)$ and $\psi_{00}(m_1, m_2)$ where the values m_1 and m_2 are the same. Thus one has by inspection of (5)

$$E_{11}(M) = g_{zz}\beta H + \tfrac{1}{2}AM + \tfrac{1}{4}(K_0 + K_z), \quad (8)$$

and

$$E_{1-1}(M) = g_{zz}\beta H - \tfrac{1}{2}AM + \tfrac{1}{4}(K_0 + K_z), \quad (9)$$

where $M = m_1 + m_2$. The remainder of the matrix is block diagonal with 2×2 blocks

$$\begin{pmatrix} \tfrac{1}{4}(K_0 - K_z) & \tfrac{1}{2}(\Delta M)A \\ \tfrac{1}{2}(\Delta M)A & -\tfrac{3}{4}K_0 - \tfrac{1}{4}K_z \end{pmatrix}, \quad (10)$$

where $\Delta M = m_1 - m_2$. The eigenvalues of (10) are

$$E^{\pm}(m_1, m_2) = -\tfrac{1}{4}(K_0 + K_z) \pm \tfrac{1}{2}A[p^2 + (\Delta M)^2]^{1/2}, \quad (11)$$

where

$$p = K_0/A. \quad (12)$$

The eigenvectors are

$$\psi^+(m_1, m_2) = \cos[\theta(\Delta M)]\psi_{10}(m_1, m_2) + \sin[\theta(\Delta M)]\psi_{00}(m_1, m_2), \quad (13a)$$

and

$$\psi^-(m_1, m_2) = -\sin[\theta(\Delta M)]\psi_{10}(m_1, m_2) + \cos[\theta(\Delta M)]\psi_{00}(m_1, m_2), \quad (13b)$$

where

$$\cot[\theta(\Delta M)] = \frac{\Delta M}{[p^2 + (\Delta M)^2]^{1/2}}. \qquad (13c)$$

If the time-dependent perturbation which induces transitions is of the form $(S_1^+ + S_2^+ + S_1^- + S_2^-)$, the transition amplitude will be zero between states that have opposite symmetry for the interchange of the two particles. The selection rules $\Delta m_1 = 0$ and $\Delta m_2 = 0$ will be exact. We shall designate those transitions between $\psi_{1\pm1}(m_1, m_2)$ and $\psi^+(m_1, m_2)$ as allowed transitions, although the term is meaningful in its usual sense only for $p \gg 1$. The frequencies of these transitions are

$$h\nu_a^{(1)}(m_1, m_2) = g_{zz}\beta H + \tfrac{1}{2}AM + \tfrac{1}{2}(K_0 + K_z)$$
$$-\tfrac{1}{2}A[p^2 + (\Delta M)^2]^{1/2}, \qquad (14a)$$

and

$$h\nu_a^{(2)}(m_1, m_2) = g_{zz}\beta H + \tfrac{1}{2}AM - \tfrac{1}{2}(K_0 + K_z)$$
$$+\tfrac{1}{2}A[p^2 + (\Delta M)^2]^{1/2}, \qquad (14b)$$

and the relative intensity of these lines is given by

$$\mathcal{I}_a = \cos^2[\theta(\Delta M)]. \qquad (14c)$$

The transitions between $\psi_{1\pm1}(m_1, m_2)$ and $\psi^-(m_1, m_2)$ shall be referred to as the forbidden transitions. Their frequencies are

$$h\nu_f^{(1)}(m_1, m_2) = g_{zz}\beta H + \tfrac{1}{2}AM + \tfrac{1}{2}(K_0 + K_z)$$
$$+\tfrac{1}{2}A[p^2 + (\Delta M)^2]^{1/2}, \qquad (15a)$$

and

$$h\nu_f^{(2)}(m_1, m_2) = g_{zz}\beta H + \tfrac{1}{2}AM - \tfrac{1}{2}(K_0 + K_z)$$
$$-\tfrac{1}{2}A[p^2 + (\Delta M)^2]^{1/2}, \qquad (15b)$$

and the relative intensity of these lines is

$$\mathcal{I}_f = \sin^2[\theta(\Delta M)]. \qquad (15c)$$

For an experiment at constant frequency, the position of these transitions on a magnetic field display will be

$$H_a^{(1)}(m_1, m_2) = H_0 + (1/g_{zz}\beta)\{-\tfrac{1}{2}(K_0 + K_z)$$
$$-\tfrac{1}{2}AM + \tfrac{1}{2}A[p^2 + (\Delta M)^2]^{1/2}\}, \qquad (16a)$$

$$H_a^{(2)}(m_1, m_2) = H_0 + (1/g_{zz}\beta)\{\tfrac{1}{2}(K_0 + K_z)$$
$$-\tfrac{1}{2}AM - \tfrac{1}{2}A[p^2 + (\Delta M)^2]^{1/2}\}, \qquad (16b)$$

$$H_f^{(1)}(m_1, m_2) = H_0 + (1/g_{zz}\beta)\{-\tfrac{1}{2}(K_0 + K_z)$$
$$-\tfrac{1}{2}A[p^2 + (\Delta M)^2]^{1/2}\}, \qquad (16c)$$

$$H_f^{(2)}(m_1, m_2) = H_0 + (1/g_{zz}\beta)\{\tfrac{1}{2}(K_0 + K_z)$$
$$-\tfrac{1}{2}AM + \tfrac{1}{2}A[p^2 + (\Delta M)^2]^{1/2}\}, \qquad (16d)$$

where $H_0 = h\nu/(g_{zz}\beta)$. If K_0 and K_z are both positive, the forbidden and allowed lines corresponding to the superscript 2 will be at high-field, and those corresponding to superscript 1 will be low-field lines. If both are negative, the reverse will hold for both the allowed and forbidden. When K_0 and K_z are comparable and of opposite sign [as occurs for a spin-spin interaction of the form $(S_1^x S_2^x + S_1^y S_2^y)$], the high- and low-field

classifications for the allowed and forbidden lines may be different.

For $K_0 = 0$, the allowed lines with a fixed value for $M - \Delta M$ coincide. This gives rise to a set of $2I + 1$ lines each of multiplicity $2I + 1$ spaced at $A/g_{zz}\beta$, shifted up and down in field by $K_z/2g_{zz}\beta$.

For $K_0 \gg A$, it is convenient to discuss the displacement of the positions $H_a^{(2)}$ and $H_f^{(2)}$ relative to

$$H_0 + \tfrac{1}{2}(K_0 + K_z)/g_{zz}\beta - \tfrac{1}{2}A(M - \Delta M)/g_{zz}\beta$$

and

$$H_0 + \tfrac{1}{2}(K_0 + K_z)/g_{zz}\beta - \tfrac{1}{2}A(M + \Delta M)/g_{zz}\beta,$$

respectively. The $\Delta M = 0$ lines are shifted down in field by $K_0/2g_{zz}$ whereas the allowed lines with $\Delta M \neq 0$ are shifted down by a smaller amount given approximately by $(K_0)^2/4g_{zz}A(\Delta M)^2$, and the corresponding forbidden lines are shifted up by the same amounts. Thus the lines with large ΔM tend to remain together as K_0 increases, the forbidden lines on one end of the spectrum and the allowed lines on the other end. For example, the allowed line with $M = 0$ and $\Delta M = 2I$, remain near the position $H_0 + \tfrac{1}{2}(K_0 + K_z)/g_{zz}\beta - IA/g_{zz}\beta$ until p is of the order of $2I$. This behavior is illustrated in Fig. 1, where two computer-generated spectra are shown for $I_1 = I_2 = (\tfrac{7}{2})$ and for two values of p. The 64-component lines were assumed to be the derivative of Gaussian curves with a peak-to-peak width of $0.17A$. The line positions were calculated from Eqs. (16b) and (16d) and the intensities from (14c) and (15c). Five of the $\Delta M = 0$ transitions can be clearly identified in Fig. 1(b) for $p = 1$, where they are shifted to lower field by $\tfrac{1}{2}K_0/g_{zz}\beta = \tfrac{1}{2}A/g_{zz}\beta$. The high-field line, which remains nearly stationary relative to positions defined at the beginning of this paragraph, is a composite of forbidden lines with large ΔM and $M - \Delta M = -7$ (if A is positive); and the second line from the low-field side is a composite of allowed transitions with large ΔM. These two features break up rather slowly as p increases beyond unity and as they do so, the intensity of the forbidden lines decreases rapidly.
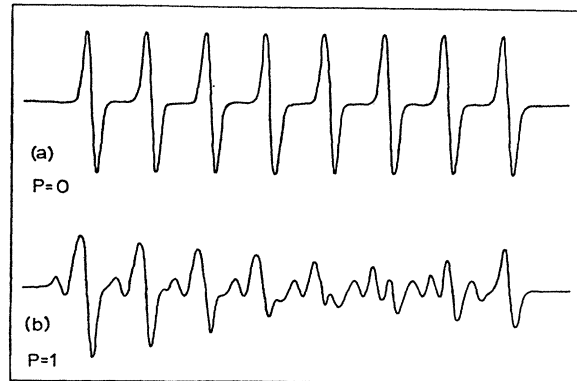
FIG. 1. Computer-generated hyperfine spectra for pairs of similar ions for $p = 0$ and $p = 1$. The individual lines are derivatives of Gauss error functions with a peak-to-peak width of $0.17A$.
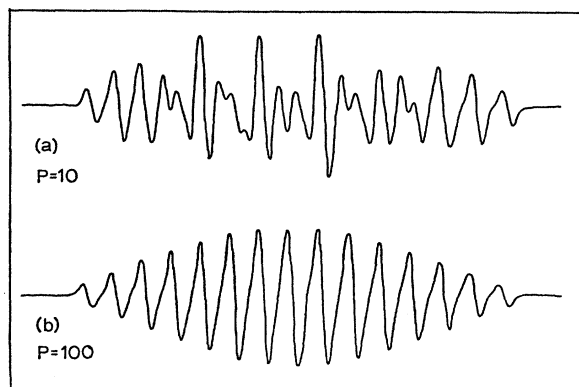
FIG. 2. Computer-generated hyperfine spectra of coupled ions for $p=10$ and $p=100$. The individual line shapes are the same as in Fig. 1.

In Fig. 2(a), a spectrum for $p=10$ is shown. This structure is almost perfectly symmetrical, because it contains only very minute contributions from the forbidden transitions. The high-field and low-field lines are $\Delta M=0$ transitions with $M=\pm 7$.

For very large p one finally obtains the stairstep structure mentioned in the Introduction. Figure 2(b) shows a spectrum for $p=100$. Careful inspection of this spectrum reveals that p is not infinite. If the lines for different ΔM, and the same M coincided exactly, the lines would be as sharp as those in Fig. 1(a) and still resolved even though the spacing is only half as large. A broadening of the central transitions is revealed by comparing the intensity of the center lines with those on the outside. If the lines were not broadened in the center (where those transitions with large ΔM must be located), the intensity ratio would be $2I$ or 7 in this case whereas the actual ratio is only 5.66. This illustrates a potentially useful technique for determining large values of K_0/A. The sensitivity clearly depends on the width of the individual hyperfine components. For large p, the shift of the lines with $M=0$, $\Delta M=0$ relative to those with $M=0$, $\Delta M=2I$ is given approximately by

$$H_a^{(1)}(I,\,-I)-H_a(0,0)\approx\frac{AI^2}{g_{zz}\beta}\frac{1}{p}\ . \quad (17)$$

Thus if this is an appreciable fraction of the linewidth for a single transition, the intensity of the derivative of the inner transitions relative to the outer ones will be measurably reduced from the value $2I$. The shift of the $M=0$, $\Delta M=2I$ transition relative to the $\Delta M=2I-2$, the next smallest ΔM consistant with $M=0$, is

$$\Delta H=\frac{A(2I-1)}{g_{zz}\beta}\frac{1}{p}\ , \quad (18)$$

and if this is about equal to a linewidth, the value of K_0 relative to A may be extracted from this splitting with useful precision.

Equations (16a)–(16d) may be quite adequate even if $B\neq 0$, but $B\gg g\beta H/I$, for then the corrections are only of the order of $(BI)^2/(g\beta)^2H$. The magnitude of these corrections is in no way appreciably greater than in the main hyperfine structure, but a pattern as complicated as that shown in Fig. 2(a) for $p=10$ may be affected by rather small shifts and some caution is advisable. If the width of the individual hyperfine lines is W, then the criterion for the neglect of the second-order hyperfine effects in the pattern simulation is that they be small compared with W.

The analysis may also be quite accurate even if the spin-spin interaction is not of axial form. Off-diagonal spin-spin terms of the form $K'(S_1^z S_2^++S_1^+S_2^z)$ shift both $H_a^{(1)}$ and $H_a^{(2)}$ down in field by an amount of the order of $(K')^2/4(g_{zz}\beta)^2H$. Such effects can be easily eliminated for lines without hyperfine structure by using the separation of the high and low pair lines as a measure of $K_z/g_{zz}\beta$. But if $p\sim 1$, the amount of shift may be different for the lines with different ΔM because the matrix elements of the spin-spin operator between $\psi^+(m_1,m_2)$ and ψ_{10} will be proportional to $\cos[\theta(\Delta M)]$, and this may distort the pattern if the differential effects for varying ΔM are of the order of W. For the forbidden lines, the relevant matrix elements are proportional to $\sin[\theta(\Delta M)]$ and similar considerations apply. If the spin-spin terms were not symmetric for the interchange of the two ions, the situation would be even more involved. In general, the rule that the second-order effects be small compared with the linewidth is ultraconservative, and one of our examples illustrates that reliable results can be obtained when the corrections are nearly equal to the width.

The signs of the interactions are determined if one knows whether the high-field pair spectrum corresponds to $H_a^{(1)}$ or $H_a^{(2)}$. This can be determined by measuring the relative intensity of the high and low pair as the temperature is varied. The set which we have designated with the superscript (2) corresponds to a transition from the ψ_{1-1} state which is the lowest of the triplet states if $|K_z|\ll 2\hbar\omega$, where ω is the observing frequency. This set will grow stronger relative to the set (1) by the factor $\exp(\hbar\omega/kT)$. If K_z or $K_0\sim 2\omega$, the discussion is a bit more complex.

III. APPLICATIONS

A. Pr³⁺ in Lanthanum Ethyl Sulfate

The arrangement of the trivalent ions in the trigonal (C_{3h}) crystal $La_2(C_2H_5SO_4)_6\cdot 9H_2O$ is shown in Fig. 3.[7] There are two types of trivalent sites which are distinguished by the fact that the environments for ions such as 1 and 3 in the figure are related by reflection in a mirror plane. Any pair of ions along the trigonal axis are identical. This fact is important because it has been shown that the EPR transitions are driven by the

[7] J. A. Ketelaar, Physica **4**, 619 (1937).
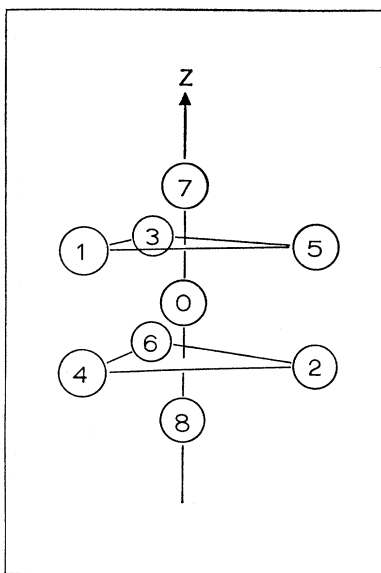
FIG. 3. The trivalent ion positions in LES and LaCl₃. The distance from 0 to 7 or from 0 to 8 is 7.11 Å in LES at room temperature and 4.366 Å in LaCl₃ at room temperature. Ions 1, 2, 3, 4, 5, 6 are at 8.11 Å in LES and 4.83 Å in LaCl₃.

electric field and the coupling has the opposite sign for sites which are mirror images of each other.[8,9] The crystal field has the symmetry C_{3h} and it leaves a doublet lowest. The spin Hamiltonian for a single ion is[10]

$$\mathcal{3C} = g_{11}\beta H_z + AI_zS_z + \Delta_xS_x + \Delta_yS_y$$
$$+\gamma E_xS_x + \gamma E_yS_y, \quad (19)$$

in which Δ_x and Δ_y describe the strain-induced splitting of the doublet and lead to the asymmetric line shapes observed for transitions between the doublets, $g_{11} = 1.672$, and for the 100%-abundant isotope ¹⁴¹Pr, $I = \frac{5}{2}$ and $A = 0.0814$ cm⁻¹. It has been shown that $\gamma = 12.4g_{11}\beta$ so that an excellent signal may be obtained if the crystal is placed in the microwave electric field. The spread of Δ_x and Δ_y (and therefore the asymmetric linewidth) depend on the concentration of Pr³⁺ primarily because of the strain induced by the misfitting of the ions in the host lattice.[10,11]

The spectrum obtained for a 1%-doped crystal at 4.2°K, with an observing frequency of 38.09 GHz, and with the magnetic field along the trigonal axis is shown in Fig. 4. This is a recording of the resonant absorption rather than the derivative. The pair lines are visible below and above the single-ion resonance which runs off the vertical scale. For reasons that are discussed in detail at the end of this subsection, we believe that this spectrum arises from the axial pair (0–7 or 0–8 in Fig. 3).

⁸ J. W. Culvahouse, D. P. Schinke, and D. Foster, Phys. Rev. Letters **18**, 117 (1967).
⁹ F. I. B. Williams, Proc. Phys. Soc. (London) **91**, 111 (1967).
¹⁰ J. M. Baker and B. Bleaney, Proc. Roy. Soc. (London) **A245**, 156 (1958).
¹¹ J. W. Culvahouse, L. Pfortmiller, and D. P. Schinke, J. Appl. Phys. **39**, 690 (1968).

It is possible to locate 42 pair lines, 21 in a low-field set and 21 in a high-field set. Each set of 21 can be classified into six subsets, the lines in each being spaced at the interval $A/g_{11}\beta$, and the number of lines in each is 6, 5, 4, 3, 2, and 1. The center of each subset is displaced from the center of the six-member subset by an amount which fits the expression

$$\delta H = (\tfrac{1}{2}Ag_{11}\beta)\{[p^2 + (\Delta M)^2]^{1/2} - p\}, \quad (20)$$

where $\Delta M = 6 - N$, N is the number in each subset, and the shift is to higher field for the high-field set and to lower field for the low-field set. The data fits $p = 5.7$, corresponding to $|K_0| = 6000$ G or 0.47 cm⁻¹. The hyperfine interval of the pairs in magnetic field units was found to be $(0.2 \pm 0.1)\%$ greater than for the single-ion spectrum. The position of the $\Delta M = 0$ lines can be used to determine K_z with great precision. The separation of the center of the high- and low-field $\Delta M = 0$ sets is 6098 ± 15 G, which gives $|K_z| = 0.474 \pm 0.001$ cm⁻¹. The mean field of these two sets of lines was 70 G greater than the center field of the single-ion spectrum. Measurements near 16 GHz showed that this shift was proportional to the field and corresponded to a change in g of -0.007, so that for the pairs $g = 1.665$, and this value has been used to convert field separations to energy units.

Careful examination of the chart from which Fig. 1 was prepared reveals 15 more lines on the high-field side, and indications of extra lines on the low-field side. These proved to be the forbidden lines, and can be seen quite clearly in Fig. 5, a derivative trace taken at 15.822 GHz and 4.2°K with a high-quality crystal.[12] The 15 forbidden lines fall into subsets of 5, 4, 3, 2, and 1 lines with an intensity increasing as the number of lines in the subset decreases. In Fig. 5, the extreme high-field lines of each allowed subset are identified by the numbers 1, 2, 3, ···, etc., and the high-field lines of each forbidden subset is labeled by the numbers 2(a), 3(a), ···, etc. The forbidden lines 1(a), corresponding to $\Delta M = 0$, have zero intensity. Each forbidden subset is shifted to lower field relative to the corresponding allowed subset by 93 ± 4 G. Inspection of Eqs. (16) shows that the separation of subsets of allowed and forbidden lines with the same ΔM by an amount which is independent of ΔM can occur only if one compares the set $H_a^{(1)}$ and $H_f^{(2)}$ or $H_f^{(1)}$ and $H_a^{(2)}$. These lines are separated by an amount $(K_0 + K_z)/g\beta$ and we may conclude that this sum is about 93 G, but one cannot determine the sign since one does not know if the high-field allowed lines correspond to $H_a^{(1)}$ or $H_a^{(2)}$. The forbidden lines on the low-field side are shifted up by 93 G as they should be, but are of lower intensity than the allowed lines. The reason for this is vividly demonstrated by observing the relative intensity of the lines

¹² The ethyl sulfate crystals partially decompose easily and such crystals show very much larger linewidths. Freshly grown crystals appear to be always superior.

FIG. 4. The absorption spectrum for LES with 1% Pr at 38.09 GHz with the field along the symmetry axis. The asymmetrical line shape is the result of random zero-field splittings. The lines of the pair spectrum are present on the low- and high-field sides and extend into the main structure.

MAGNETIC FIELD IN KILOGAUSS
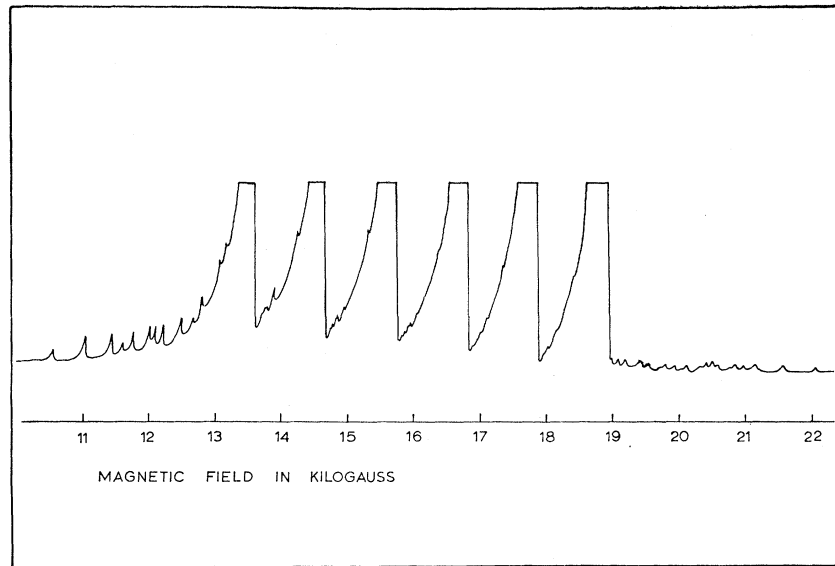
as the temperature is lowered to 1.2°K. The high-field forbidden lines become increasingly stronger than the low-field forbidden lines and the high-field allowed lines become increasingly weaker than the low-field allowed lines. This implies that the high-field sets correspond to $H_a^{(1)}$ and $H_f^{(2)}$. Therefore, $K_z = -0.474$ and $K_0 = +0.467$. The sum, $(K_0+K_z)=J_{00}$, is -0.0073 cm^{-1}. This implies that the spin-spin interaction is almost precisely of the "planar" form

$$\mathcal{K} = -J_{1-1}(S_1{}^x S_2{}^x + S_1{}^y S_2{}^y) + J_{00} S_1{}^z S_2{}^z, \quad (20)$$

with $J_{1-1} = -0.467$ and $J_{00} = -0.0073$. The measurements, of course, are not very sensitive to off-diagonal terms in the spin-spin interaction. An off-diagonal term with a coefficient 0.03 cm^{-1} would produce a downward shift of the centroid of the pairs of about 10 G at 15.9 GHz and would be just at the limit of detectibility. If $g_\perp$ were not zero, the presence of other terms could be detected with great sensitivity by making measurements with the magnetic field in other directions. Most important, if the pair were not an axial pair the spectrum would split up into several components and these would change their relative positions if the crystal were rotated about the c axis with the magnetic field at some nonzero angle with that axis. In the present case, all that a perpendicular component of the field does is to admix some of the excited states into the ground doublet. We have observed some of these effects on the pair spectrum and more lines are resolved, but the spectrum remains axially symmetric for rotations about the c axis. An even more compelling reason for believing that these spectra are due to the axial pair is the great sensitivity of the doublets to strains with symmetry lower than trigonal which introduce a zero-field splitting Δ that would shift the spectrum to lower field by $\Delta^2/(2\hbar\omega g_{||}\beta)$. It is very unlikely that a nearby nonaxial

Pr^{3+} would not produce an observable effect by this mechanism. It has been observed that the asymmetric linewidth is greater for low concentrations of Pr^{3+} than for full concentrations, and that this effect is even more dramatic for Pr^{3+} in YES where there is a greater degree of misfit of the Pr^{3+} in the lattice.[10,11] We have made similar, although slightly less accurate, measurements on this pair in YES, and found no greater downward shift. It appears quite conclusive that this spectrum is that of the axial pair, and it is probable that the near-neighbor nonaxial pairs correspond to such a large zero-field splitting that they cannot be observed even with a frequency of 38 GHz. This assumption also explains our failure in other experiments to observe pairs in double nitrate crystals doped with Pr^{3+} where there are no sites for close axial pairs.

If these are axial pairs, our classification of the
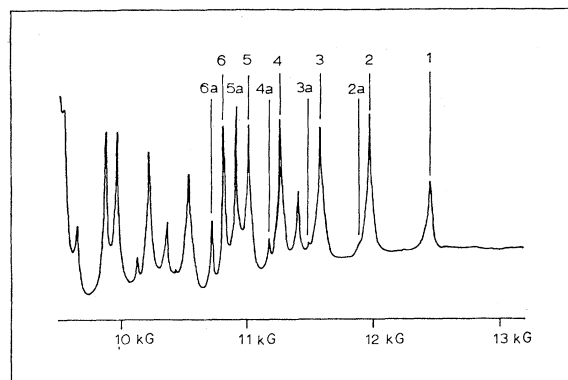
FIG. 5. A derivative of absorption for LES doped with 1% Pr at 15.822 GHz taken on the high-field side of the isolated ion resonance. The first line of each ΔM subset is identified and numbered 1, 2, $\cdots$, 6. The corresponding forbidden lines are numbered 2a, 3a, $\cdots$, 6a. Line 1a would be a forbidden line with $\Delta M = 0$ and has zero intensity.

TABLE I. Data for the axial pairs investigated in this paper. Both the axial pair coefficients K_0 and K_z and the spherical tensor coefficients J_{00} and J_{1-1} are tabulated when the knowledge of the signs permits. Signs are printed explicitly when known. Energy units are cm^{-1}. δg is listed only for $g_{||}$.

Ion crystal	K_0	K_z	J_{00}	J_{1-1}	Nondipolar part $J_{00}{}^{(nd)}$	$J_{1-1}{}^{(nd)}$	$g_{||}$	A (10^4 cm^{-1})	$\delta g_{||}$	δA (10^4 cm^{-1})
Pr^{3+} LES	+0.467 ±0.001	−0.474 ±0.001	−0.0073 ±0.0003	−0.467 ±0.001	−0.0004 ±0.0003	−0.467 ±0.001	1.665 ±0.001	815 ±0.5	0.007 ±0.001	1.0
Pr^{3+} LaCl$_3$	2.44 ±0.25	1.79 ±0.01								
Co^{2+} LMN	+0.105 ±0.003	−0.170 ±0.003	−0.065 ±0.003	−0.105 ±0.003	+0.064 ±0.004	−0.040 ±0.004	4.31 ±0.02	95.5 ±1.0	0.25 ±0.02	17.1 ±2

forbidden and allowed transitions on the basis of intensity behavior is correct because γ has the same sign for both members of the pair. Had γ been of the opposite sign for the two ions, our classification would have been inverted, and the values K_0 and K_z interchanged from their true values.

It is also unlikely that this spectrum is due to second nearest-neighbor axial pairs, since the nearest-neighbor axial pairs would have to have an interaction less than 0.01 cm^{-1} or greater than 5.0 cm^{-1} in order to explain our failure to observe them. A large interaction is incompatible with low-temperature specific-heat data, and the small value is unlikely.

The axial pair is separated by 7.11 Å, and the dipolar interaction is

$$(J_{00})^{(d)} = -2(g_{||}\beta)^2/4r^3 = -0.0067 \text{ cm}^{-1},$$

$$(J_{1-1})^{(d)} = 0.$$

Since the Pr^{3+} ions are smaller and the lattice is at low temperature, it appears that the dipole-dipole interaction could easily be larger than the value calculated with the room temperature lattice constant 7.11 Å. Baker[13] quotes a private communication from Hopkins stating that the lattice constant is smaller by 1% at 4.2°. With this correction the dipolar value is −0.0069 cm^{-1}, virtually within our probable rrror.

The dominant form of the interaction is the pure planar form and as we will demonstrate in another paper,[6] the planar interaction of the nearest-neighbor axial pairs is quite adequate to explain the major aspects of the low-temperature specific heat and a spread of Δ as used by Meyer[14] is no longer required. This form is also consistent with either an electric multipole or a phonon exchange source for the interaction. The values of the constants are summarized in Table I.

B. Pr^{3+} in Anhydrous Lanthanum Trichloride

The trivalent ion lattice of LaCl$_3$ is identical to that of the ethyl sulfate except for the lattice parameters. The separation of the axial pair in this material is only 4.37 Å,[15] and one may anticipate much larger spin-spin

interactions, an expectation that is reenforced by the low-temperature specific-heat measurements.[16] The spin Hamiltonian constants from our measurements are as follows: $g_{||} = 1.029 \pm 0.003$ and $A = 0.0505 \pm 0.0002$ cm^{-1}.

Measurements on a crystal doped with 1% Pr^{3+} and at a frequency of 36.63 GHz showed one line of the main spectrum within our field range at 22.90 kG, and a pair spectrum centered at 6.94 kG. This pair spectrum is shown as a derivative of absorption in Fig. 6(a). It is apparent that this is a structure corresponding to a rather large value of p. Some structure is resolved in the center just below the $M=0$ peak. This is the most prominent extra feature and is due to the $\Delta M = 5$ transition. Several smaller bumps are discernable which are due to the $\Delta M = 4$ transitions. The separation of the $\Delta M = 5$ and $\Delta M = 4$ transitions can be estimated grossly from the chart and the value of p calculated from Eq. (18). One obtains values of 40–70 in this way. Rather precise results may be obtained by using a line shape which represents the central portion of the derivative of a single line quite accurately, and generating from that shape a complete spectrum with the use of Eqs. (16). There are several matching criteria which one can use, but one of the most sensitive is the ratio of the separation of the high-field peak of the $\Delta M = 5$ transition from the unresolved high-field $M=0$ peak to the separation of the unresolved high-field peaks due to the $M=0$ and $M=1$ lines. These features are indicated in Fig. 6a by arrows. This criterion and others that we have used leads to $p=48\pm4$ or $K_0=2.44\pm0.25$ cm^{-1}. A simulated spectrum for $p=48$ is shown in Fig. 6(b). The structure is reproduced quite well, and the over-all appearance would have been better had the individual line-shape function been more accurate in the tail of the lines. The positions of the peaks, however, are quite insensitive to the behavior of the tail which is quite smooth.

Using the hyperfine interval for the main spectrum that was measured at 16 GHz, we may infer that the center of the isolated ion resonance would be at 25.53 kG. This if we ignore the possibility of a g shift for the pairs, the magnitude of $K_z/(2g_{||}\beta)$ is either 25.53–6.94 or 25.53+6.94 kG. The correct alternative was de-

[13] J. M. Baker and A. E. Mau, Can. J. Phys. **45**, 403 (1967).
[14] Horst Meyer, J. Phys. Chem. Solids **9**, 296 (1959).
[15] W. A. Zachariasen, Acta Cryst. **1**, 265 (1948).

[16] J. H. Colwell and B. W. Mangum, J. Appl. Phys. **38**, 1468 (1967).
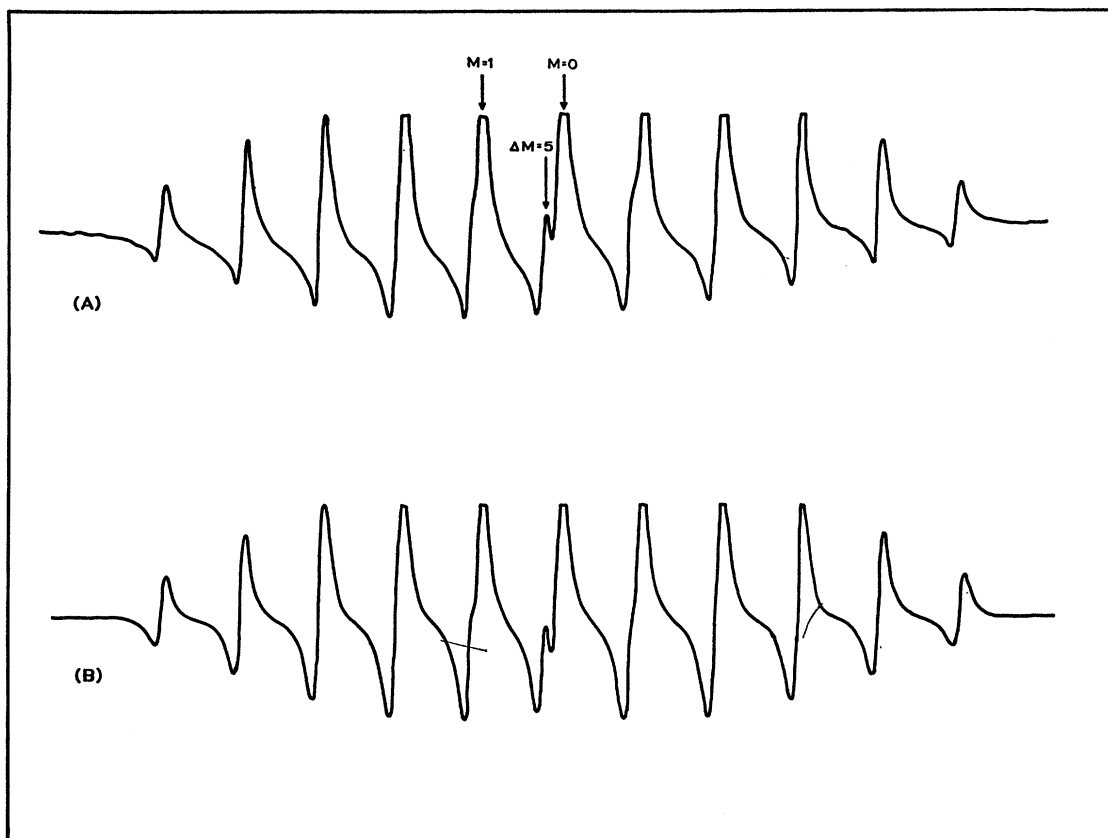
FIG. 6. (a) The pair spectra of 1% Pr in $LaCl_3$ measured at 36.63 GHz. The $\Delta M = 5$ transition and two other positions used for a criterion of fit are identified by arrows. (b) The computer-generated spectrum for $p = 48$ and an approximate shape for the component lines.

termined from measurements at 36.94 GHz for which the center of the pair spectrum was at 7.18 kG. This is quite adequate to show that K_z is less than $2\hbar\omega$ so that the magnitude of $K_z/(g_{11}\beta)$ is 37.2±0.1 kG. This frequency change is so small and our accuracy of frequency measurement so gross in this range that we can only quote that for the pairs $g_{11} = 0.90 \pm 0.20$. The g shift should be determined by measurements near 16 GHz, but the pairs then fall among lines of the isolated spectrum or on the low side where the asymmetric line shape leads to a large amount of overlap. Measurements below 12 GHz should show a number of the pair lines above the isolated ion spectrum. The hyperfine interval of the pairs measured in magnetic field units at 36 GHz is 1.1% greater than that measured for the isolated ion spectrum at 16 GHz. Since there is no reason for the (A/g) value of the isolated ion to change significantly with increasing magnetic field along the symmetry axis, this difference is attributable to a difference between the pairs and the single ions. The significance of the change in this ratio could be better assessed if the magnitude of the g shift were known with precision.

The determination of the signs of the spin-spin interaction coefficients in this case is far more difficult than when the spin-spin interactions are smaller. The for-

bidden transitions cannot be seen so the simple determination of the relative sign of K_0 and K_z from that data is not possible. We have compared the intensity of the pair spectrum with that of an isolated ion as a function of temperature between 4.2° and 1.5°. The ratio of the intensity of the isolated resonance to the intensity of the pairs was 1.38 times greater at 4.2°K than at 1.5°K. To avoid nonlinearities from excessive perturbation of the microwave cavity, the pair resonance was compared with the isolated ion resonance of Pr^{3+} in a very small double nitrate crystal, and care was taken to avoid saturation of either resonance.

We label the four possible sign combinations as follows: Case I; $K_0 > 0$, $K_z < 0$. Case II; $K_0 < 0$, $K_z > 0$. Case III; $K_0 > 0$, $K_z > 0$. Case IV; $K_0 < 0$, $K_z < 0$. The predicted values for the experimental measurement described in the last paragraph are 0.62, 1.21, 0.32, and 1.21. Thus our experiment favors case II or IV. If the axial pair interaction is the dominant one in $PrCl_3$, the measurements of the specific heat and susceptibility by Colwell and Mangum[16] are helpful. Cases III and IV correspond to an anisotropic exchange that is in the range for which Bonner and Fisher[17] have calculated the

---

[17] Jill C. Bonner and Michael E. Fisher, Phys. Rev. **135A**, 640 (1964).

thermodynamic properties of linear chains. They write the spin-spin interaction in the form

$$\mathfrak{IC} = -2J[S_1{}^z S_2{}^z + \gamma(S_1{}^x S_2{}^x + S_1{}^y S_2{}^y)]. \quad (21)$$

Cases III and IV correspond to $\gamma = 0.55$ and $J = \mp 2.21$ cm^{-1}. The broad specific-heat peak for the antiferromagnetic case III would be at 2°K rather than the 0.8°K observed. The specific-heat peak for the ferromagnetic case IV would be very close to the experimental value, but the predicted behavior of the susceptibility is much different from the experimental results. Our cases I and II correspond to $\gamma = -3.75$ and are close to the pure planar case evaluated by Katsura.[18] For the constants measured by us, the specific-heat peak is predicted to be at 1.05°. Considering the size of the nonplanar term for PrCl$_3$, the agreement is encouraging. We should logically conclude that case II is the most likely. However, there is only a factor of 2 difference in the predicted intensity variation for cases I and II, an unsatisfactory margin of error in such an involved experiment. We have therefore listed no sign for the interaction coefficients in Table I, and cannot give values for J_{00} and J_{1-1}. The EPR intensity experiment needs to be repeated with lower temperatures.

C. Pairs of Co²⁺ in Double Nitrate Crystals

The spatial arrangement of the divalent ions nearest an X-ion site in the double nitrate crystals is shown in Fig. 7. The interionic distances given in the caption are those determined by Zalkin et al.,[19] for Ce₂Mg₃ (NO₃)₁₂·24H₂O. The pair interactions reported here were measured for Co²⁺ in La₂Mg₃(NO₃)₁₂·24H₂O, hereafter designated LMN. Only the interaction of the nearest-neighbor X-X pair (0-1, in Fig. 7) is discussed here because it provides a different example of the analysis of the hyperfine structure of pairs. For the X-Y pairs, the g factors are quite different, and the pair spectra can be studied under conditions such that the hyperfine structure of the pairs are simple replicas of the single-ion hyperfine structure.

The single-ion Hamiltonian for Co²⁺ is

$$\mathfrak{IC} = g_{\parallel}\beta S_z H_z + g_{\perp}\beta(S_x H_x + S_y H_y)$$
$$+ A I_z S_z + B(I_x S_x + I_y S_y). \quad (22)$$

For the X site of LMN, $g_{\parallel} = 4.06$, $g_{\perp} = 4.45$, for the 100%-abundant isotope ⁵⁹Co, $A = 78.4 \times 10^{-4}$ and $B = 104.2 \times 10^{-4}$ cm^{-1}. For the Y site, $g_{\parallel} = 7.36$, $g_{\perp} = 2.337$, $A = 292 \times 10^{-4}$, and $B \leq 3 \times 10^{-4}$ cm^{-1}.

The analysis of the X-X pair spectra is complicated because in addition to the X-X pair spectra about an isolated X-ion spectrum, there is another spectrum due to X ions with a Y-ion neighbor. A detailed study is made possible only because $g_{\parallel} = 4.31 \pm 0.02$ and $g_{\perp} = 4.32 \pm 0.02$ for the X-X pairs, whereas the g values

[18] Shigetoshi Katsura, Phys. Rev. **127**, 1508 (1962).
[19] Allan Zalkin, J. D. Forrester, and David H. Templeton, J. Chem. Phys. **39**, 2881 (1963).
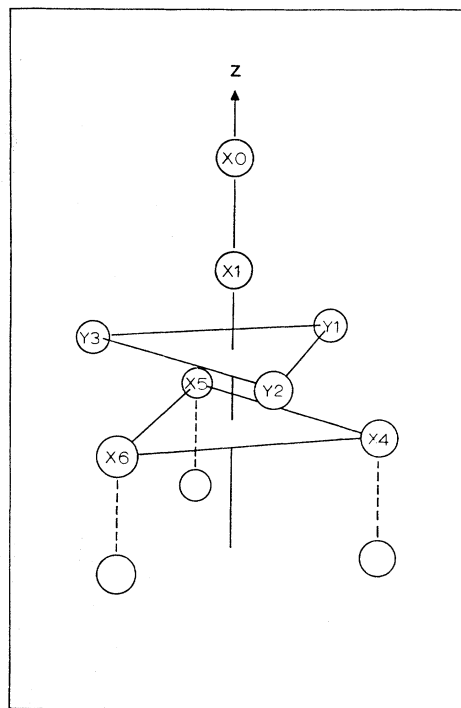
FIG. 7. The divalent ion environment of an X ion in LMN. The distance $X0$-$X1$ is 4.99 Å. The next-nearest neighbors are Y ions at 7.15 Å.

of the X-Y pairs are much nearer to those for the isolated ion. Thus with the field along the symmetry axis and an observing frequency of 37.42 GHz, the low-field X-X pair spectrum is below the low-field spectrum of X ions with a Y-ion neighbor, and is well above the isolated Y-ion spectrum and the spectra of the Y ions with magnetic neighbors. The X-X pair spectrum under these conditions is shown in Fig. 8(a) for a sample with a 1:100 Co to Mg ratio. On the high-field side, above the dashed line, some of the spectrum of the X-X pairs is obscured by the first lines of an eight-line hyperfine structure due to X ions with Y-ion neighbors. The corresponding high-field X-X pair spectrum lies under the main spectrum. The multiplicity of lines in the spectrum suggest an intermediate value of p, of the order of 10. In Fig. 8(b), we show a spectrum generated for $p = 11.3$ using individual lines of Gaussian shape and a peak-to-peak width W of 8 G, in agreement with the width of the isolated ion resonances. The hyperfine interval $A/g_{\parallel}\beta$ was adjusted to 47.5 G so to reproduce the distance between the lowest-field line and the highest-field line that is not obscured by the X-Y pair spectra. The detail of the agreement of the two spectra is quite remarkable, and the residual difference could be due to the second-order hyperfine effects which can shift the lines 1 or 2 G relative to each other. Other spectra generated for slightly different p values imply $p = 11.3 \pm 0.5$.

The extreme high-field and extreme low-field lines of

the generated spectrum correspond to $M=7$. The center of the pair spectrum is therefore $\frac{7}{2}A/g_{11}\beta$ G above the low-field line. The center of the isolated ion resonance is at $h\nu/g_{11}'\beta$, where g_{11}' is the isolated ion g factor. We measure this center field to be 6603 G for an observing frequency of 37.42 GHz. The low-field line of the X-X pairs is at 5622 G, 931 G below the center of the isolated ion spectrum. From Eqs. (16), we have

$$931 = \frac{K_z}{2g_{11}\beta} + \frac{7}{2}\frac{A}{g_{11}\beta} + 6603\left(1 - \frac{g_{11}'}{g_{11}}\right). \quad (23)$$

Where the last term arises from the difference of the g factors. At 16.412, the $M=7$ line at 2132 G is still clear of the X-Y pairs and the isolated ion resonance is at 2880 G. Thus, we have

$$757 = \frac{K_z}{2g_{11}\beta} + \frac{7}{2}\frac{A}{g_{11}\beta} + 2889\left(1 - \frac{g_{11}'}{g_{11}}\right). \quad (24)$$

These two equations are quite accurate theoretical expressions because the spin-spin interaction is rigorously of the form (1) and the second-order hyperfine corrections are quite negligible. The solution of (23) and (24) yields $K_z/g_{11}\beta = 836 \pm 15$ G and $g_{11} = 4.31 \pm 0.02$, where the errors reflect the combined errors of the several field measurements and the effect of the imprecise value of A. The value of p determined by fitting the shape of the X-X pair structure yields the value $K_0/g_{11}\beta = 537 \pm 30$ G and $A = (95.5 \pm 1.0) \times 10^{-4}$ cm^{-1}. Culvahouse et al.[20] have shown that for Co^{2+} in these sites, the value of g_{11} and A are simply related. The result can be written

$$A = (95.8 \pm 0.5) \times 10^{-4}[1 + 3(1 - g_{11}/4.33)]. \quad (25)$$
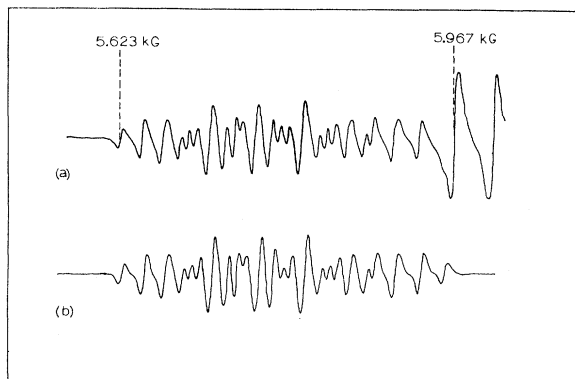
FIG. 8. (a) The spectrum of X-X pairs of Co^{2+} in LMN for the magnetic field along the symmetry axis and an observing frequency of 37.42 GHz. The two large lines on the high-field side are a part of the spectrum of X-Y pairs. (b) A computer-generated spectrum for $p=11.3$ and a linewidth for the component lines of 8 G.

[20] J. W. Culvahouse, Wesley P. Unruh, and David K. Brice, Phys. Rev. **129**, 2430 (1963).
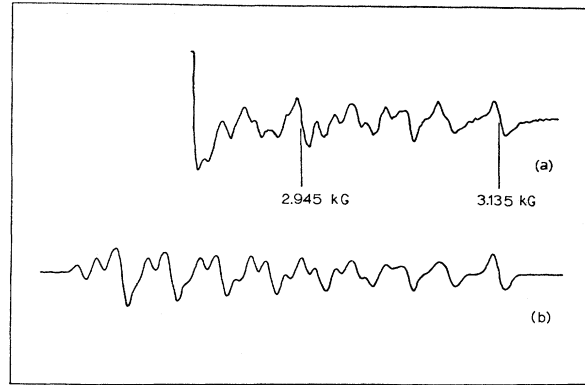
FIG. 9. The spectrum of X-X pairs of Co^{2+} in LMN for the magnetic field perpendicular to the symmetry axis and an observing frequency of 16.412 GHz. The X-Y spectra begins at the extreme left. (b) A computer-generated spectrum for $p=1.95$ and a component linewidth of 10 G.

The values of A and g_{11} found for the X-X pairs is therefore consistent with this result.

The relative sign of K_z and K_0 cannot be determined from measurements with H along the symmetry axis since the forbidden transitions are too weak to be observed, but this information can be obtained from observations with the magnetic field perpendicular to the symmetry axis. Using a direction perpendicular to the symmetry axis for the quantization axis, the spin-spin interaction assumes the form

$$\mathfrak{IC}_{ss} = K_0^{(1)}(S_1 \cdot S_2) + K_z^{(1)}S_1^z S_2^z + \frac{1}{2}K'(S_1^+S_2^+ + S_1^-S_2^-), \quad (26)$$

where

$$K_0^{(1)} = \frac{1}{2}(2K_0 + K_z), \quad K_z^{(1)} = -\frac{1}{2}K_z, \quad (27)$$

and

$$K' = \frac{1}{2}K_z. \quad (28)$$

Using the known value of K_z, the effect of the nonaxial terms can be calculated, and at 13.5 GHz we find the downward shift produced by these terms is 9 G. This is important because again we cannot observe both the high and low pairs and thus eliminate this effect. The X-X spectrum on the high side of the isolated X-ion resonance is shown in Fig. 9(a) for an observing frequency of 16.412 GHz. The g factor of the pairs is now smaller than that of the isolated ion which is expected from another relation given by Culvahouse et al. (Ref. 20) $g_{11} + 2g_\perp = 12.99 \pm 0.03$. The amount of the spectrum which can be observed is increased by the fact that the X-Y pairs which are indicated on the low side of the experimental spectrum are pushed to lower field by a strong second-order effect of the X-Y interaction. The result is that more of the spectrum can be seen clearly at 16.412 GHz than at 37.42 GHz. The X-X spectrum can be positively identified here because it is axially symmetric. The X-Y pair spectra show a sixfold periodicity, as the field direction is rotated in the basal plane and the spectrum in Fig. 9(a) was taken

with the field in the direction which produced a minimum separation of the X-Y pairs.

If one uses the values of K_z and K_0 determined from the parallel spectrum, then the value of $p_\perp = K_0^{(1)}/B$ is 2.4 ± 1.0 if K_z and K_0 have opposite signs or 19 ± 1 if they have the same signs. The second alternative can be dispensed with by casual examination of the observed spectrum. Figure 9(b) is a computer-generated spectrum for $p_\perp = 1.95$, a hyperfine interval $B/g\beta = 50$ G, and a linewidth of 10 G, comparable to that of the isolated ion resonance linewidth. The value of $B/g_\perp\beta$ was chosen to fit the positions of key points on the 200 G of observable X-X spectrum. The quality of fit is noticeably worse for 2.5% variations in $p_\perp$ or B. In view of the possible effect of nonuniform second-order hyperfine and spin-spin terms somewhat larger confidence limits are indicated, $p_\perp = 2.0 \pm 0.1$ and $B/g_\perp\beta = 49.5 \pm 1.5$. This value of $p_\perp$ definitely shows that K_0 and K_z have the opposite sign and implies $|2K_0 + K_z|/g_\perp\beta = 198 \pm 12$ G.

An independent determination of K_0 can be made and the value of $g_\perp$ determined by comparison of the spectra at 13.49 and 37.42 GHz with the field perpendicular to the symmetry axis. The high-field line of the X-X spectra are easily identified at both frequencies and the separations of the lines from the center of the isolated ion resonance are measured to be 483 ± 4 and 605 ± 10 G, and the isolated ion centers are at 2175 and 6020 G. The high-field line of the X-X spectrum is a composite of forbidden transitions with $(M \pm \Delta M) = -7$, and the strongest contributions are from the large values of ΔM. The computed spectra show that the zero crossing of this line is given quite accurately by the position of the $\Delta M = 7$ forbidden transition,

$$\tfrac{1}{2}(K_0^{(1)} + K_z^{(1)}) + (B/2g_\perp\beta)[p^2 + (7)^2]^{1/2}$$
$$= \tfrac{1}{2}(K_0^{(1)} + K_z^{(1)}) + 179.$$

The second-order shift from the term with coefficient K' is 9 G at 13.49 GHz and 3 G at 37.42. Assuming the g factor of the isolated ion to be $g_\perp'$, we have two relations to satisfy

$$313 = \tfrac{1}{2}(K_0^{(1)} + K_z^{(1)}) + 2175(1 - g_\perp'/g_\perp),$$
and
$$429 = \tfrac{1}{2}(K_0^{(1)} + K_z^{(1)}) + 6020(1 - g_\perp'/g_\perp).$$

From them we obtain $|K_0^{(1)} + K_z^{(1)}|/2g_\perp\beta = 500 \pm 20$, and $g_\perp = 4.32 \pm 0.02$. This result implies $K_0/g_{\parallel}\beta = 510 \pm 25$ G, which agrees with the determination from p within the cumulative error. The values in cm^{-1} given in Table I correspond to taking $|K_z/g_{\parallel}\beta| = 845$ G and $|K_0/g_{\parallel}\beta| = 523$ G. These results give $p = 11.0$, $p_\perp = 2.0$. While all of the measurements are fit within the confidence limits assigned, there is a tendency for the agreement to consistently be just within the limits. It is quite possible that there are field-dependent effects not included in this analysis. In view of the small splitting of the excited state of Co^{2+} (about 400 cm^{-1}),[20] it is not

unlikely that there are additional field-dependent effects which produce 5- or 10-G discrepancies in the measured separations. Any such effects lie within the errors which we quote in Table I.

The absolute signs of the interaction coefficients were determined from the temperature dependence of intensity for the high- and low-field pairs with the magnetic field parallel to the symmetry axis, and an observing frequency of 16.5 GHz. It was possible under these conditions to observe a portion of the X-X pair spectra between the isolated ion spectrum and the X-Y pair spectra on both the high- and low-field sides. Confidence in our identification was possible only after the X-X pair spectra had been fit with a theoretical shape. The most obvious measurement of the sign is afforded by the direct comparison of the low- and high-field lines. The isolated ion resonance was so strong relative to the X-X pairs that a crystal large enough to give a good signal to noise for the pairs caused the spectrometer to become unlocked from the signal cavity as the isolated ion resonance was traversed. We verified that it was possible to relock with a reproducible gain and obtained good results showing K_z to be negative. A determination which circumvented the problem of reproducible gain was made by comparison of the X-X pairs on either side with the X-Y pairs on the same side. These results showed that K_z was of the opposite sign for the X-X and X-Y pairs. The sign of the X-Y interaction was found to be positive from measurements on the much stronger X-Y pairs with a much smaller crystal so that the spectrometer remained locked to the cavity as the isolated ion resonance was traversed.

Using the separation of 4.99 Å for the X-X pairs and the experimentally determined g factors, the dipolar interactions are

$$K_0^{(d)} = +0.065 \text{ cm}^{-1}$$
and
$$K_z^{(d)} = -0.194 \text{ cm}^{-1}.$$

Thus the nondipolar contributions are

$$K_0^{(nd)} = +0.040$$
and
$$K_z^{(nd)} = +0.024.$$

The nondipolar contributions are antiferromagnetic as expected from superexchange and definitely anisotropic. The final data are summarized in Table I.

IV. CONCLUSIONS

The four examples presented here represent the major part of the spectrum of possible values for the ratio of the isotropic exchange to hyperfine splitting. The principles and techniques illustrated here are the same for all nuclear spins. The successful application of the techniques depends upon adequate resolution of the structure and use of the general trends of the hyperfine structure as illustrated in Figs. 1 and 2.